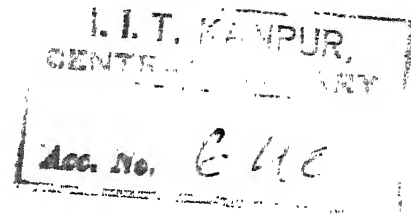# EXPERIMENTAL VERIFICATION OF DYNAMIC SHEAR ANGLE APPROACH FOR THE DETERMINATION OF STABILITY CHART

A Thesis Submitted

In Partial Fulfilment of the Requirements
for the Degree of

MASTER OF TECHNOLOGY

BY

VISHNU BHAGWAN

to the

DEPARTMENT OF MECHANICAL ENGINEERING
INDIAN INSTITUTE OF TECHNOLOGY KANPUR
DECEMBER 1971

ACKNOWLEDGEMENTS

CERTIFICATE

This is to certify that the thesis entitled "Verification of Dynamic Shear Angle Approach for the Determination of Stability Chart" has been carried out under my supervision and this work has not been submitted elsewhere for award of a degree.

DR. G.S. KAINTH
Assistant Professor
Department of Mechanical Engineering
Indian Institute of Technology Kanpur

DECEMBER 1, 1971

TABLE OF CONTENTS

SYNOPSIS

The present work is aimed to verify the dynamic shear angle approach for the prediction of stability chart.

A flexible tool holder is designed and fabricated. The flexibility of the tool holder is much higher in the horizontal direction as compared to the vertical direction so that the machine tool workpiece system is assumed to be a single degree of freedom system. Response locus of the tool holder is determined by exciting the tool holder in the horizontal direction and measuring its response in the same direction.

Experimental stability chart is obtained by machining hot finished seamless M.S. tube on L.B.25 Lathe using throw-away-tip-type carbide tools.

A computer program is developed to solve the equations of threshold of stability. Theoretical stability chart is obtained using the computed results.

Experimental stability chart shows a close agreement with theoretical results above cutting velocity 70 m.p.m. when the builtup edge is insignificant.

LIST OF NOTATIONS

A_c Amplitude of Incremental Tangential Cutting Force

A_s Shear Plane Area

A_t Amplitude of Incremental Thrust Force

a_1 Amplitude of Tool Oscillation

a_2 Amplitude of wave on Uncut Surface of the workpiece

C Cutting Coefficient $= (D \cos f - 1)/D \sin \emptyset$

D Stress Ratio $= \dfrac{T_c}{T_s}$

d Diameter

dF_c Incremental Tangential Cutting Force

dF_t Incremental Thrust Force

ds Change in Instantaneous Uncut Chip-Thickness

ds_1 Tool Oscillation

ds_2 Wave form of Uncut Surface of Work

$d\alpha$ Change in Rake Angle

F_c Tangential or Main Cutting Force

F_{ci} Instantaneous Cutting Force in Instantaneous Cutting Direction

F_{cim} Instantaneous Cutting Force in Mean Cutting Direction

F_t Thrust Force

F_{ti} Instantaneous Thrust Force Component Normal to Instantaneous Direction of Cutting

F_{tim} Instantaneous Thrust Force Component Normal to Mean Direction of Cutting

f Frequency in Cycles per Second

G   Mean Geometric Lead

G_i Instantaneous Geometric Lead

K_1 $Gn_1 + n_2$

L_1 Length of Chip Before Cutting

L_2 Length of Chip After Cutting

n_1 Shear Angle-Chip Thickness Coefficient $= \partial\phi/\partial s$

n_2 Shear Angle-Rake Angle Coefficient $= \partial\phi/\partial\alpha$

r   Mean Radius of Workpiece

R   Resultant Force

s   Mean Uncut Chip-Thickness

s_i Instantaneous Uncut Chip Thickness

s_1 Uncut Chip Thickness (Feed Rate)

s_2 Cut Chip Thickness

T   Time Period Per Revolution, Vibration Period

T_c Cutting Stress

T_s Shearing Stress

t   Time

v,V   Mean Cutting Speed

X   Distance Measured in the Normal Direction to Machined Surface

α Mean Rake Angle

α_1 Instantaneous Rake Angle

β Angle of Friction at Rake Face of Tool

β_i Angle Between Mean and Instantaneous Direction of Cutting

γ Mean Angular lead of Free End of Shear Plane

γ_i Instantaneous Angular Lead of Free End of Shear Plane

θ Phasing Between Uncut Surface Waveform and Tool Oscillation

λ Wave Length

μ Overlap Factor .

$\emptyset$ Mean Shear Angle

$\emptyset_i$ Instantaneous Shear Angle Referred to Instantaneous Cutting Direction

ψ_c Phase of Incremental Tangential Cutting Force

ψ_t Phase of Incremental Thrust Force

ω Angular Speed in Radians Per Second.

CHAPTER 1

INTRODUCTION

Metal cutting process is often associated with vibrations between tool and work piece. These vibrations cause poor surface finish, reduce tool-life, affect machining accuracy and reduce production rate.

Three types of vibrations occur in machine tools:

(a) Forced vibrations are caused by the unbalancing effects in the machine tool work piece system.

(b) Free vibrations are caused due to the shock transmitted through the foundation from the neighbouring machines.

(c) Self excited vibrations are also called chatter vibrations. Chatter is caused by interaction of cutting process with the dynamic behaviour of the machine tool structure.

Forced and free vibrations are well understood and can be eliminated easily. Chatter vibrations pose a greater problem. These vibrations are due to the dynamic instability of the machine tool system.

In order to predict the dynamic stability region of machine tool system, one has to analyse :

(a) Dynamics of machine Tool Structure, and

(b) Dynamics of Cutting process.

1.1 Dynamics of machine Tool Structure

Dynamic behaviour of a structure is represented by harmonic response locus of the structure. The response of the machine tool structure in the direction of applied harmonic exciting force is called the direct response of the structure. Direct response per unit force is termed direct receptance.

The response of the structure in the direction perpendicular to the applied harmonic exciting force is termed the cross response of the structure. Cross response per unit force is called the cross receptance.

The receptance of a structure can be represented by a complex number, (a+ib). (Ref. 1,2). Where a represents the inphase component of receptance and b represents the out of phase component of the receptance. If (a+ib) is plotted in such a way that 'a' is plotted as abcissa and 'b' as ordinate, then the harmonic receptance locus is obtained.

1.2 Dynamics of Cutting Process

During chatter vibration, the tool vibrates relative to the work piece and cutting parameters such as depth of cut, rake angle and cutting speed etc., undergo

cyclic vibration which lead to non-steady-state metal cutting.

Tlusty and Polacek (Ref.3) assumed that variation in cutting forces depends only upon the chip thickness variation caused by relative vibration of tool and workpiece.

Tobias and Fishnick (Ref.4) assumed that variation in cutting forces under dynamic cutting conditions depends upon chip thickness variation, cutting speed variation and tool penetration rate.

Das (Ref.5,6) used the concept of universal machinability index for predicting the dynamic cutting forces. He also considered that shear plane does not vary under dynamic cutting conditions.

Knight (Ref.7) used the results of Das and Tobias (Ref.6) for the prediction of the stability of a simplified machine tool system.

The previous research workers have tried to predict the dynamic cutting forces from the characteristics of steady state cutting forces. However the theoretical analysis has not shown satisfactory agreement with experimental results.

Kainth (Ref.8) gave a theoretical model for predicting dynamic forces from the results of the steady state cutting tests. He considered the shear plane length as the most influential parameter in the steady state metal cutting.Considering dynamic shear angle, he gave a model (Fig.1) of dynamic cutting forces from which the expressions for incremental tangential cutting force dF_c and incremental thrust force dF_t can be written as follows :

$$dF_c = A_c \; Sin \; (\omega t + \psi_c) \qquad (1.1)$$

$$dF_t = A_t \; Sin \; (\omega t + \psi_t) \qquad (1.2)$$

where,

A_c = Amplitude of the incremental cutting force dF_c

$$= \left[\begin{array}{c} \{A_{c1} \; Cos \; \psi_{c1} - A_{c2} \; Cos(\theta + \psi_{c2})\}^2 \\ + \{A_{c1} \; Sin \; \psi_{c1} - A_{c2} \; Sin(\theta + \psi_{c2})\}^2 \end{array} \right]^{\frac{1}{2}} \qquad (1.3)$$

ψ_c = Phase angle of the Incremental cutting force.

$$= \arctan \left[\frac{A_{c1} \; Sin \; \psi_{c1} - A_{c2} \; Sin \; (\theta + \psi_{c2})}{A_{c1} \; Cos \; \psi_{c1} - A_{c2} \; Cos \; (\theta + \psi_{c2})} \right] \qquad (1.4)$$

Wave on Work $\dfrac{ds_2}{\theta}$

CHIP

$\dfrac{\lambda}{2}$

$da - \alpha$

α_i

l_i

TOOL

l_s

Tool Oscillation

ds_1'

ds_2

s

ds_1

ϕ_i

ϕ_{im}

l_s

e

Direction of Increasing ds_1 and ds_2

$G_i\beta_i$

β_i

G_i

o

b

c

F_{ci}

F_{ti}

WORK
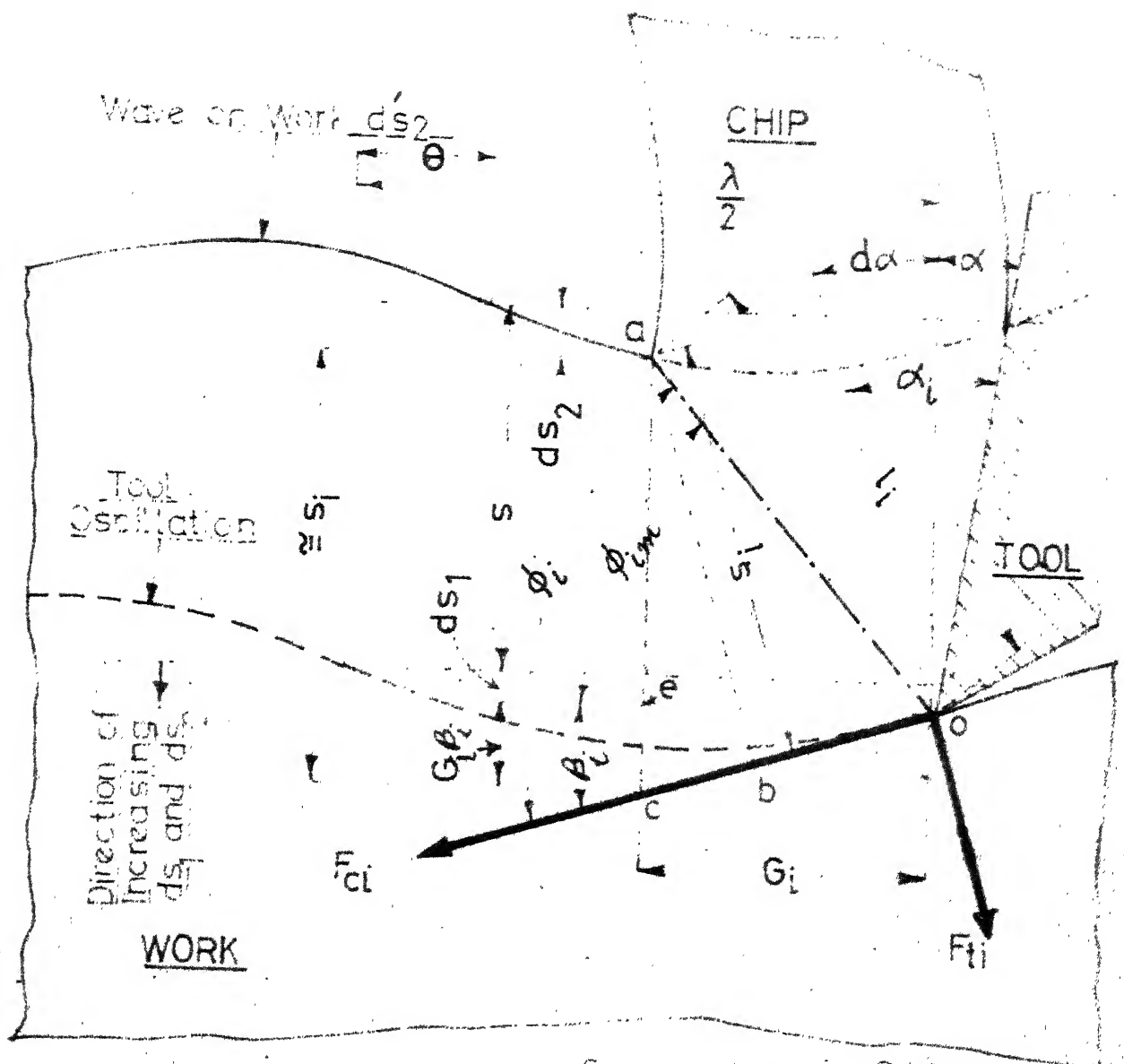
$s_i = s + ds_1 - ds_2 + G_i\beta_i$

s = mean chip thickness

$ds_1 = a_1 \sin \omega t$

$\phi_{im} = \phi_i - \beta_i$

$\gamma_i = \dfrac{2\pi G_i}{\lambda}$

$ds_2 = a_2 \sin(\omega t + \theta + \gamma_i)$

GEOMETRY OF DYNAMIC CUTTING

(WAVE - ON - WAVE CUTTING)

FIG. 1

A_t = Amplitude of the incremental thrust force

$$= \left[\begin{array}{c} \{A_{t1} \cos \psi_{t1} - A_{t2} \cos (\theta + \psi_{t2})\}^2 \\ + \{A_{t1} \sin \psi_{t1} - A_{t2} \sin (\theta + \psi_{t2})\}^2 \end{array} \right]^{\frac{1}{2}} \quad (1.5)$$

ψ_t = Phase angle of the incremental thrust force

$$= \arctan \left[\frac{A_{t1} \sin \psi_{t1} - A_{t2} \sin (\theta + \psi_{t2})}{A_{t1} \cos \psi_{t1} - A_{t2} \cos (\theta + \psi_{t2})} \right] \quad (1.6)$$

Phase angles ψ_c and ψ_t are relative to the oscillation of the tool.

$$A_{c1} = \frac{T_c W n_1}{\sin \emptyset} \sqrt{(1 - n_1 s \cot \emptyset)^2 + \{(1 - K_1) \cot \emptyset - c\}^2}$$
$$(2 \pi s / \lambda)^2 \quad (1.7)$$

$$\psi_{c1} = \arctan \left[\frac{\{(1 - K_1) \cot \emptyset - c\}\{(2 \pi s / \lambda)\}}{1 - n_1 s \cot \emptyset} \right] \quad (1.8)$$

$$A_{t1} = \frac{T_c W n_2}{\sin \emptyset} \sqrt{ \{c - n_1 s (1 + 2c \cot \emptyset)\}^2 + }$$
$$\{(1 + c \cot \emptyset) - K_1 (1 + 2c \cot \emptyset)\}^2$$
$$(2 \pi s / \lambda)^2 \quad (1.9)$$

$$\psi_{t1} = \arctan \left[\frac{\{(1 + c \cot \emptyset) - K_1 (1 + 2 c \cot \emptyset)\} 2 \pi s / \lambda}{c - n_1 s (1 + 2c \cot \emptyset)} \right]$$
$$(1.10)$$

$$\Delta_{c2} = \frac{T_c \, Wa_2}{\sin \emptyset} (1 - n_1 \, s \, \cot \emptyset) \tag{1.11}$$

$$\psi_{c2} = \quad -2\pi \, . \quad 2\pi \, s \, \cot \emptyset \, /\lambda \tag{1.12}$$

$$\Delta_{t2} = \frac{T_c \, Wa_2}{\sin \emptyset} \left\{ c - n_1 \, s \, (1 + 2c \, \cot \emptyset) \right\} \tag{1.13}$$

$$\psi_{t2} = \gamma \quad -2\pi \quad 2\pi \, s \, \cot \emptyset /\lambda \tag{1.14}$$

Kainth carried out experiments to measure dynamic cutting forces and showed good correlation between experimental and theoretical results.

1.3 Determination of Threshold of Stability

Under the presence of chatter vibration, cutting forces $(F_c + dF_c)$ and $(F_t + dF_t)$ act on the system as shown in Fig. 2.

Knight (Ref.7) gave the following expression for the displacement of tool in x-direction :
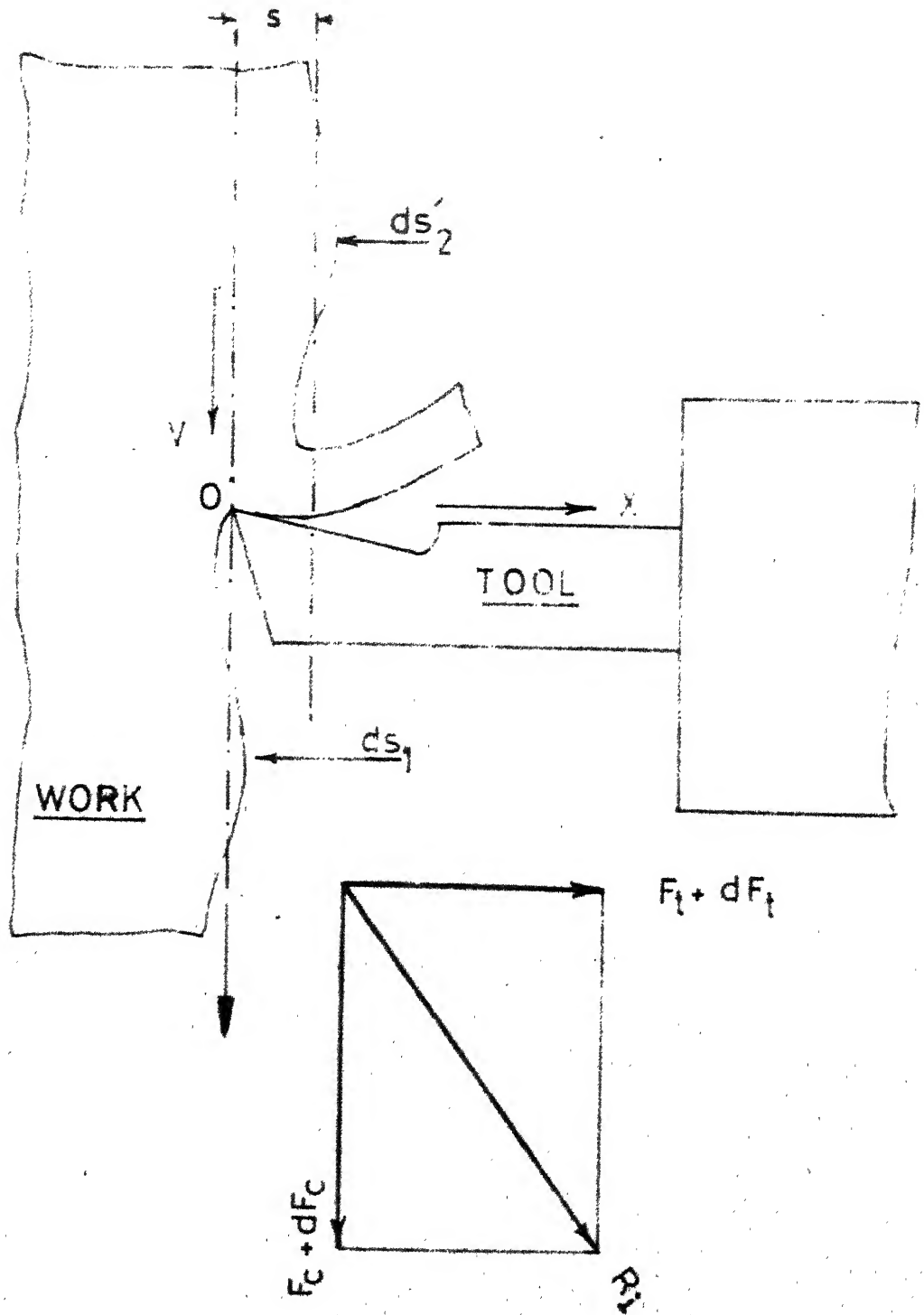
$$\bar{X}(t) = - (g + ih) \, dF_t - (p + iq) \, dF_c \tag{1.15}$$

where,

$(g + ih)$ = direct receptance of structure

$(p + iq)$ = cross receptance of structure

At the threshold of stability, vibration magnitude will remain constant irrespective of time.

NOMENCLATURE of CUTTING PROCESS

FIG.2

Hence vibration can be written in the form,

$$X(\tau) = A_O \, e^{i\omega t} \tag{1.16}$$

$$= ds_1$$

= tool vibration

$$ds_2' = A_O \, e^{i\omega(t-T)} \tag{1.17}$$

= wave generated on the work piece

$$ds_2 = A_O \, e^{i\omega(t-T) + \gamma} \tag{1.18}$$

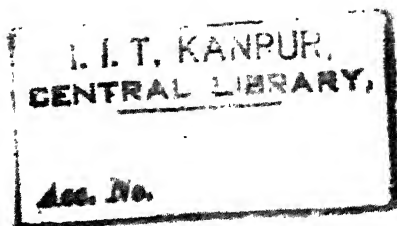= value of ds_2' at a mean angular lead of γ

ahead of tool point 'O'

Kainth (Ref.8) used his analysis to solve equation

(1.15) and gave the following conditions for the threshold of

stability :

$$
\begin{aligned}
1 = & -\frac{T_c W}{\text{Sin } \emptyset} (g + ih)
\left[
\begin{aligned}
& \{c - n_1 s (1 + 2c \text{ Cot } \emptyset)\} \\
& (1 - \mu \text{ Cos } \theta' + i \mu \text{ Sin } \theta') \\
& + \frac{i\omega s}{V} \{(1 + c \text{ cot } \emptyset) \\
& - K_1(1 + 2c \text{ Cot } \emptyset)\}
\end{aligned}
\right] \\[2ex]
& -\frac{T_c W}{\text{Sin } \emptyset}(p + iq)
\left[
\begin{aligned}
& (1 - n_1 s \text{ Cot } \emptyset)(1 - \mu \text{ Cos } \theta' \\
& + i \mu \text{ Sin } \theta') + \frac{i\omega s}{V} \\
& \{(1 - K_1) \text{ Cot } \emptyset - c\}
\end{aligned}
\right] \tag{1.19}
\end{aligned}
$$

In equation (1.19) real and imaginary parts can be put to zero separately,

$$\frac{1}{W} = -\frac{T_c}{\sin\emptyset}
\left[
\begin{array}{l}
g(1-\mu\cos\theta')-h\,\mu\sin\theta')\left\{c-n_1 s(1+2c\cot\emptyset)\right\} \\[4pt]
-\,h\,\frac{\omega\,s}{V}\left\{(1+c\cot\emptyset)-K_1(1+2\,c\cot\emptyset)\right\} \\[4pt]
+\left\{p(1-\mu\cos\theta')-q\,\mu\sin\theta'\right\}(1-n_1 s\cot\emptyset) \\[4pt]
-\,q\,\frac{\omega\,s}{V}\left\{(1-K_1)\cot\emptyset - c\right\}
\end{array}
\right]
\tag{1.20}$$

$$0 =
\left[
\begin{array}{l}
\left\{h(1-\mu\cos\theta')+ c\,\mu\sin\theta'\right\}\left\{c-n_1 s(1+2c\cot\emptyset)\right\} \\[4pt]
+\,\frac{\omega\,s}{V}\left\{(1+c\cot\emptyset)-K_1(1+2c\cot\emptyset)\right\} \\[4pt]
+\left\{q(1-\mu\cos\theta') + p\,\mu\sin\theta'\right\}(1-n_1 s\cot\emptyset) \\[4pt]
+\,\frac{p\,\omega\,s}{V}\left\{(1-K_1)\cot\emptyset - c\right\}
\end{array}
\right]
\tag{1.21}$$

CHAPTER 2

EXPERIMENTAL INVESTIGATION OF THE STABILITY CHART

2.1 Introduction

Present work is aimed to verify the dynamic shear angle approach for the prediction of stability of machine tools from the results of steady state cutting tests. For analytical simplicity a flexible tool holder is designed such that it is essentially a single degree of freedom system. Direct harmonic response locus of the tool holder is obtained by exciting the tool holder by an electromagnetic shaker. Stability chart is determined by carrying out cutting tests on H.M.T. L.B.-25 Lathe.

2.2 Flexible Tool Holder

A flexible tool holder is designed and fabricated as shown in Fig. 3. Tool is secured in a block which is mounted on four leaf springs. Each leaf spring is screwed with the base of the tool holder at two points. This ensures rigid fixing of the leaf springs with the base of the tool holder. Other ends of the leaf springs are screwed with the block carrying the tool.

Head of the tool holder is joined to the block with the help of four bolts. By changing the mass of the head, supported on the leaf springs the natural frequency of the tool holder can be changed.

640

Leaf springs are designed in a manner such that the section modulus of these springs in y-direction is sixteen times the section modulus in x-direction. This is done to ensure that the tool holder is essentially a single degree of freedom system.

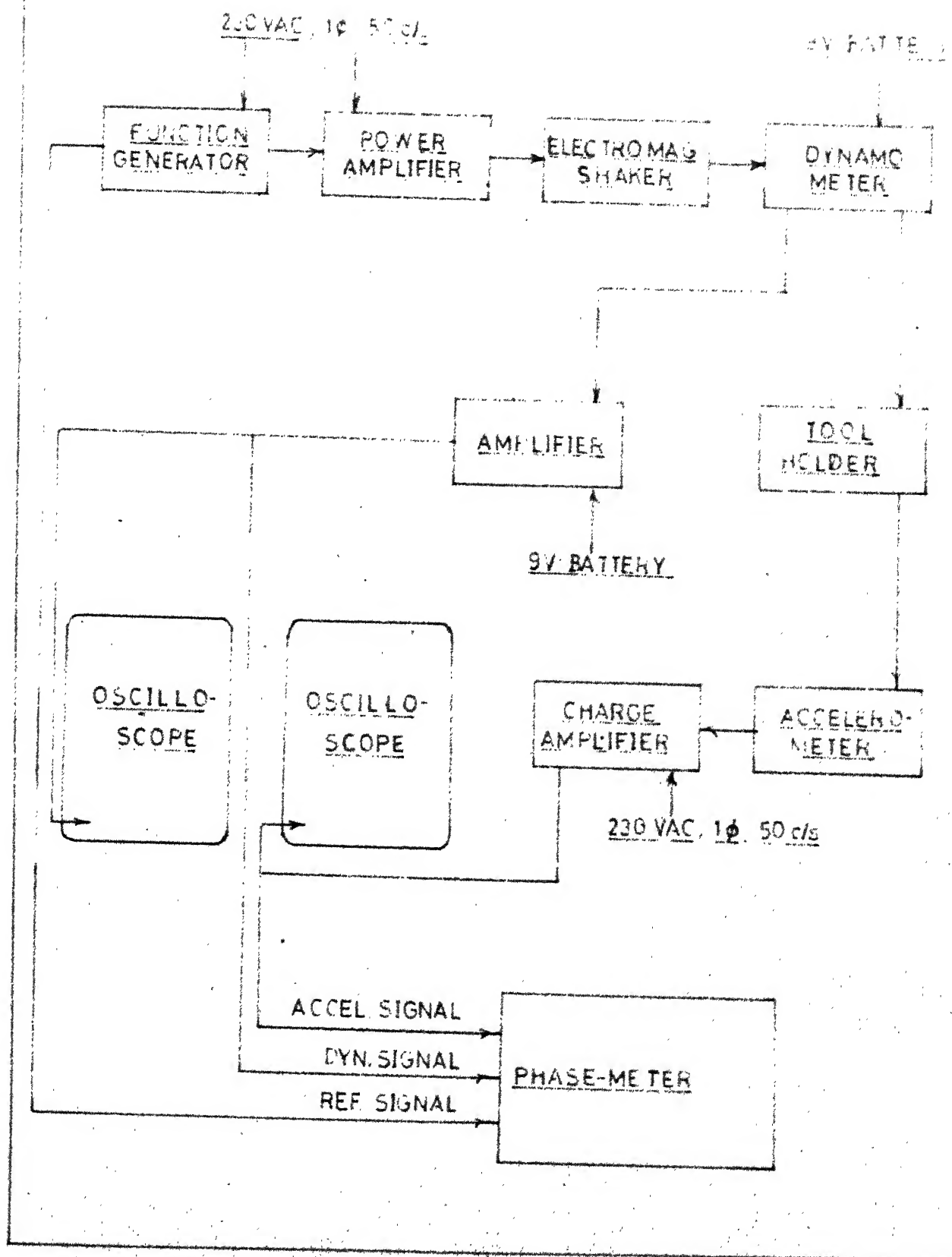## 2.2.1 Response Locus of the Tool Holder

Harmonic response locus of the tool holder is required for solving the equations of threshold of stability. This is determined by exciting the tool holder in x-direction and measuring the output of the tool holder in the same direction.

The block diagram of the instrumentation used is shown in Fig. 4. Photograph of the set up is shown in Fig. 5.

The electromagnetic shaker is placed in horizontal direction and is clamped to the base plate by a metal strip. To measure the force amplitude a dynamometer* is connected with the shaker through a right hand and left hand bolt. Lock nuts are provided to ensure the rigid fixing of dynamometer with the shaker. A mild steel bar threaded at both ends is used to connect the dynamometer with the tool holder. Tool holder is rigidly fixed with base plate through four bolts.

Sinusoidal input to the shaker is provided by a function generator through a power amplifier.

----

* Dynamometer designed by Loomba (Ref.9) was used.

BLOCK DIAGRAM of THE INSTRUMENTATION USED for RESPONSE LOCUS of THE TOOL HOLDER
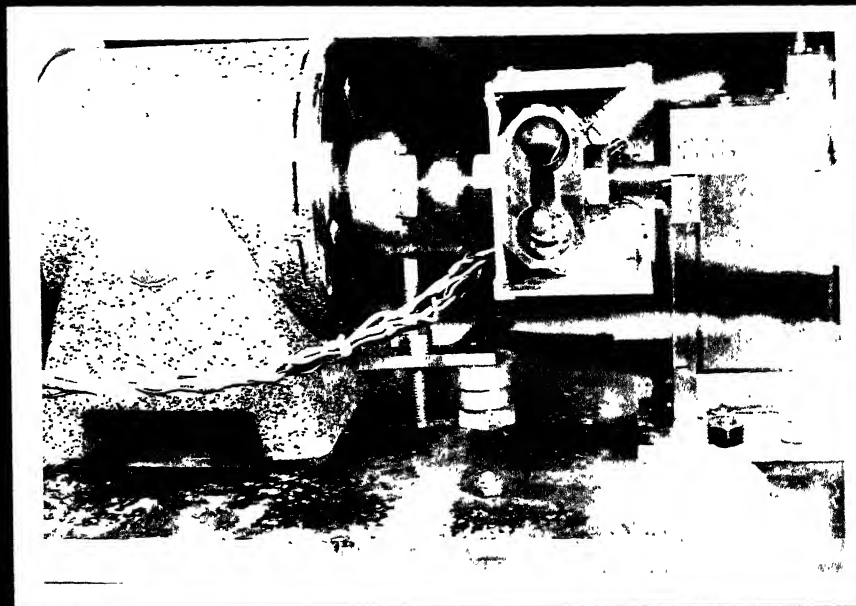
FIG.4

FIG. 5 — SET UP FOR RESPONSE LOCUS OF THE TOOL—HOLDER

A tri-axial accelerometer is fixed on the top of the tool holder to measure vibrations of the tool holder in all the three directions. Output of the accelerometer is amplified in a charge amplifier and displayed on an oscilloscope.

Dynamometer is calibrated statically by using standard weights. Calibration curve of the dynamometer is shown in Fig. 6. Cross response of the dynamometer in z direction was found to be negligible.

Phase difference between the input and the output signals can be determined by a phase-meter provided both the signals are of required magnitude. The reference signal should be above 22 V, pk-pk. and the other signal termed as input signal should be above 16 mV, pk-pk. In the present case dynamometer signal is of the order of a fraction of millivolts and accelerometer signal is of the order of a few hundred millivolts. Dynamometer signal is amplified by an amplifier having amplification factor of 400. The phase characteristic of the amplifier is determined seperately and is shown in Fig. 7.

Phase difference between the dynamometer signal and the accelerometer signal is computed after measuring the phase difference of the two signals seperately with respect to a reference signal. Reference signal is taken from the function generator.
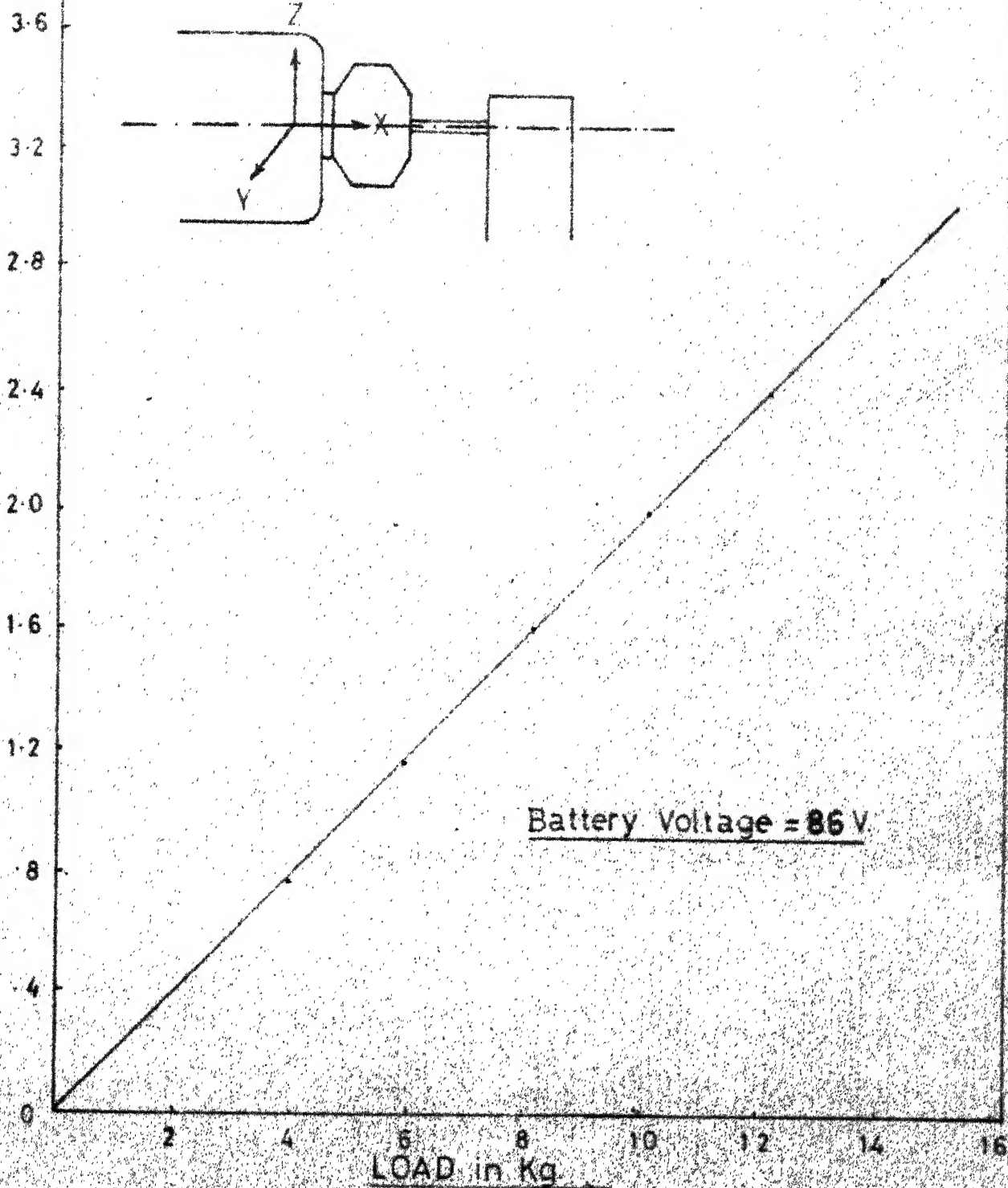
CALIBRATION of DYNAMOMETER IN X-DIRECTION

FIG 6
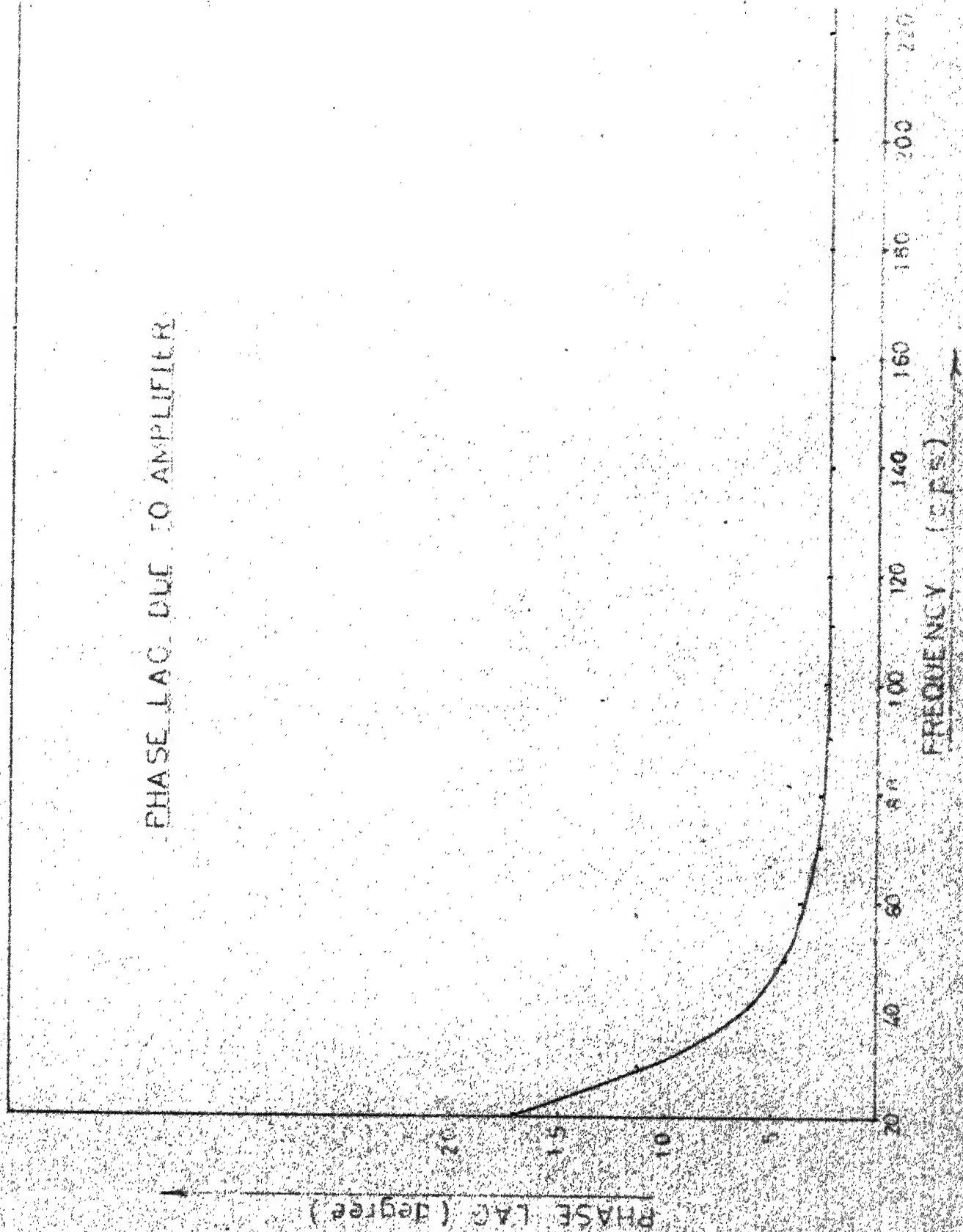
PHASE LAG DUE TO AMPLIFIER

FIG.7

2.2.2 Procedure

All the instruments are switched on, for 10 to 15 minutes, for stabilising the instruments before conducting experiment.

Force level of the shaker is kept constant at 7.5 kg.pk. which corresponds to 3 mV pk-pk output signal of the dynamometer. The signal is displayed on the oscilloscope and its amplitude is adjusted by varying the input to the shaker.

For a particular frequency, the force level is first adjusted. Output of the accelerometer in the direction of excitation is read from the oscilloscope. Inphase and quadrature components of the dynamometer signal and of the accelerometer signal with respect to the reference signal are measured seperately by the phasemeter. The procedure is repeated by seeping the frequency in steps of 2.5 cps.

Phase difference between the dynamometer signal and accelerometer signal is computed by substracting the measured phase differences of one signal from the other signal. Displacement signal leads the acceleration signal by 180°. An account of it is made while computing the phase difference. Phase shift in the dynamometer amplifier is also taken into account.

As the exciting signal is harmonic, displacement is determined by dividing the amplitude of the accelerometer signal by ω^2, where ω is the exciting frequency.

The output of the accelerometer in the two directions other than the direction of excitation is below 5 percent of the output in the direction of excitation. Hence the tool holder can be considered, essentially, a single degree of freedom system.

Inphase component of the accelerometer output is plotted as abcissa and the out of phase component of the accelerometer signal is plotted as ordinate. The frequency of oscillation is indicated along the curve. The curve thus obtained is called the harmonic response locus of the tool holder and is shown in Fig. 8.

2.3 Experimental Stability Chart

For determining stability chart experimentally, H.M.T. L.E.-25 Lathe being very sturdy is selected. As the tool-holder is much more flexible in x-direction as compared to y-direction, hence the machine tool work piece system can be assumed to be a single degree of freedom system.

The photographs of the experimental set up are shown in Fig. 9 and Fig. 10.

For determining stability regions closer steps of speed, as compared to the steps available with L.E.-25, are desired. For obtaining closer steps of speeds, motor of the lathe is replaced by a continuous variable speed D.C.Motor.

IN PHASE RESPONSE, Cm/Kg. X 10^{-4}
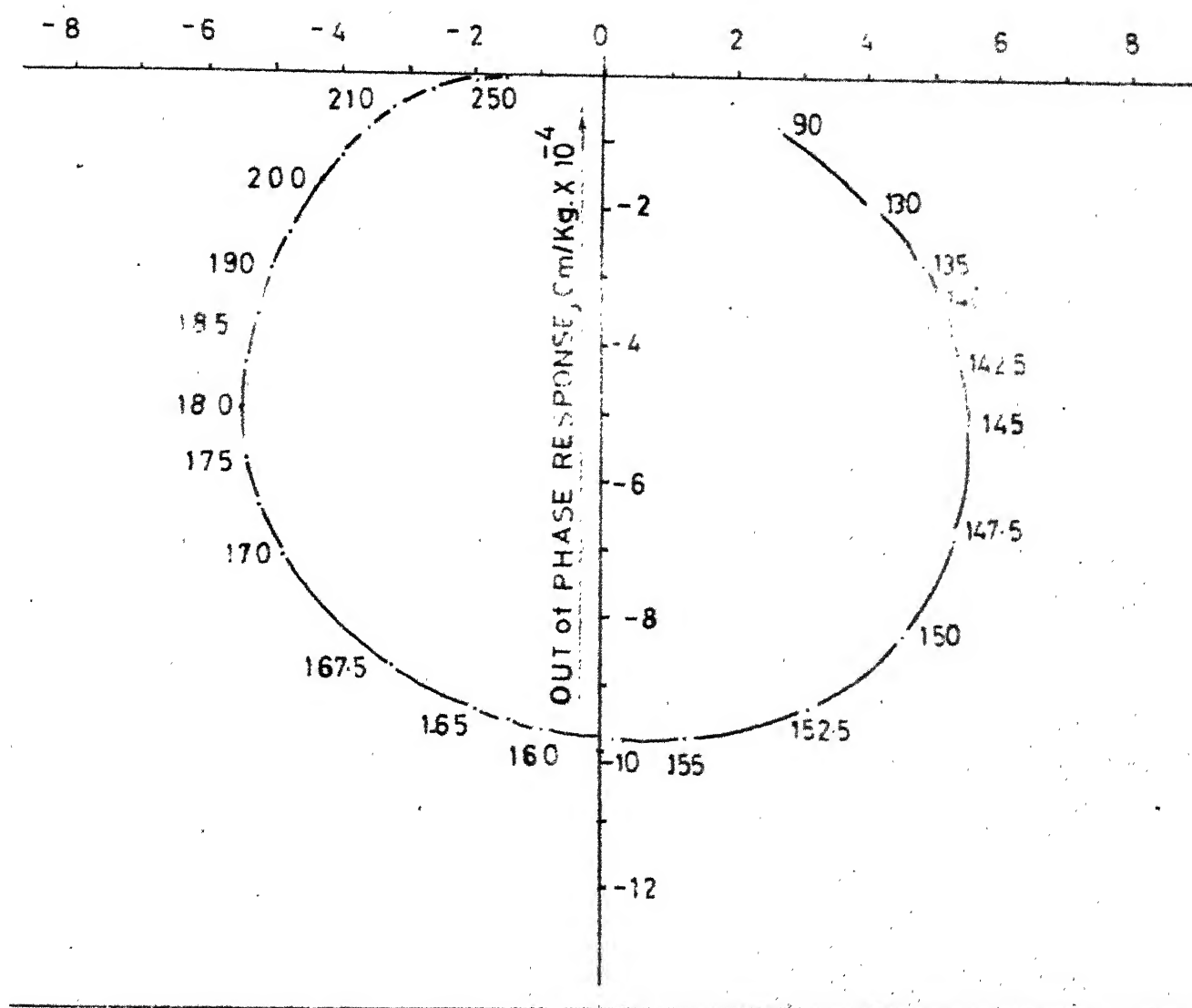
RESPONSE LOCUS of THE FLEXIBLE TOOL HOLDER

FIG.8

FIG. 9 - SET UP FOR EXPERIMENTAL STABILITY CHART

FIG. 10 - INSTRUMENTATION FOR EXPERIMENTAL STABILITY CHART

A special mounting is designed and fabricated for this purpose.
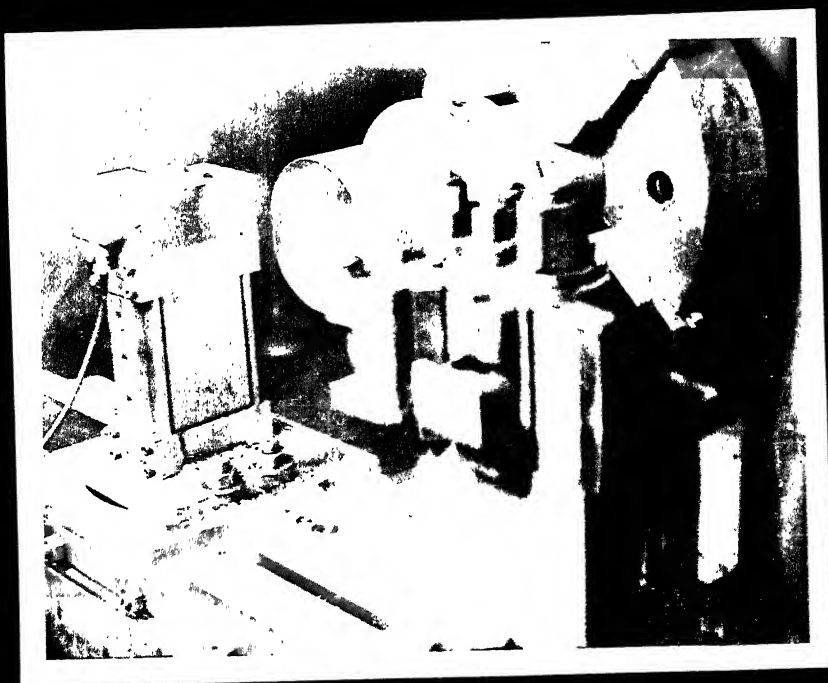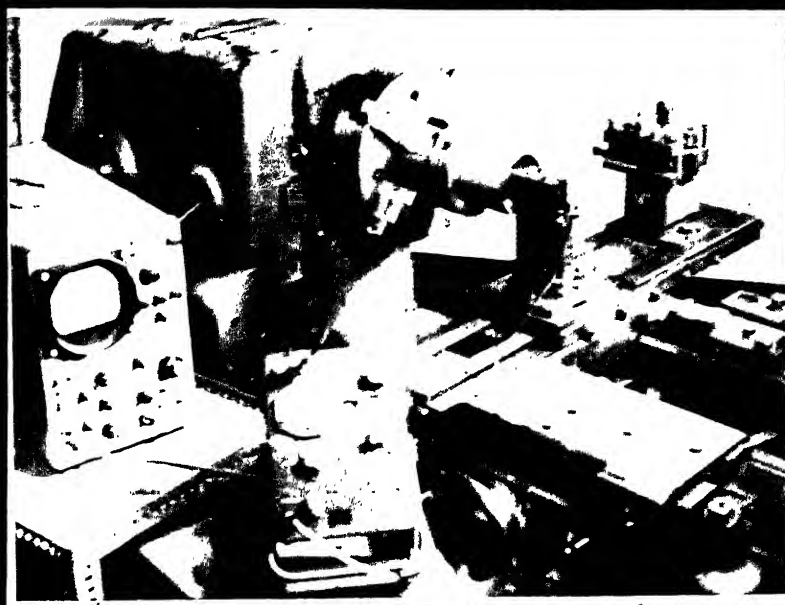
Hot finished seamless M.S. tube having .25% carbon was used for experiment. Carbide throw-away-tool-tips with 5° rake angle were used for machining tube specimens of 8" length at a feed of .05 mm per revolution. Higher feeds could not be used due to the lower capacity of the variable speed motor as compared to the standard motor supplied with the lathe.

2.3.1 Instrumentation

Block diagram of the instrumentation used is shown in Fig. 11. A vibration pick up is attached at the back of the tool holder. The pick up is suitable for a frequency range of 2-20000 cps. The pick up is connected to the vibration-meter for measuring the magnitude of the vibration. Output of the vibration meter is displayed on the storage oscilloscope for measuring its frequency.

A techometer is used to measure the speed of the driving motor. Spindle speed of the lathe is computed by knowing the gear ratio and the speed of the original motor.

2.3.2 Procedure

Tube specimens of 8" length are turned with a mean radius of 54 mm. Work piece is mounted in the adopter which is used to avoid the centering of individual pieces.
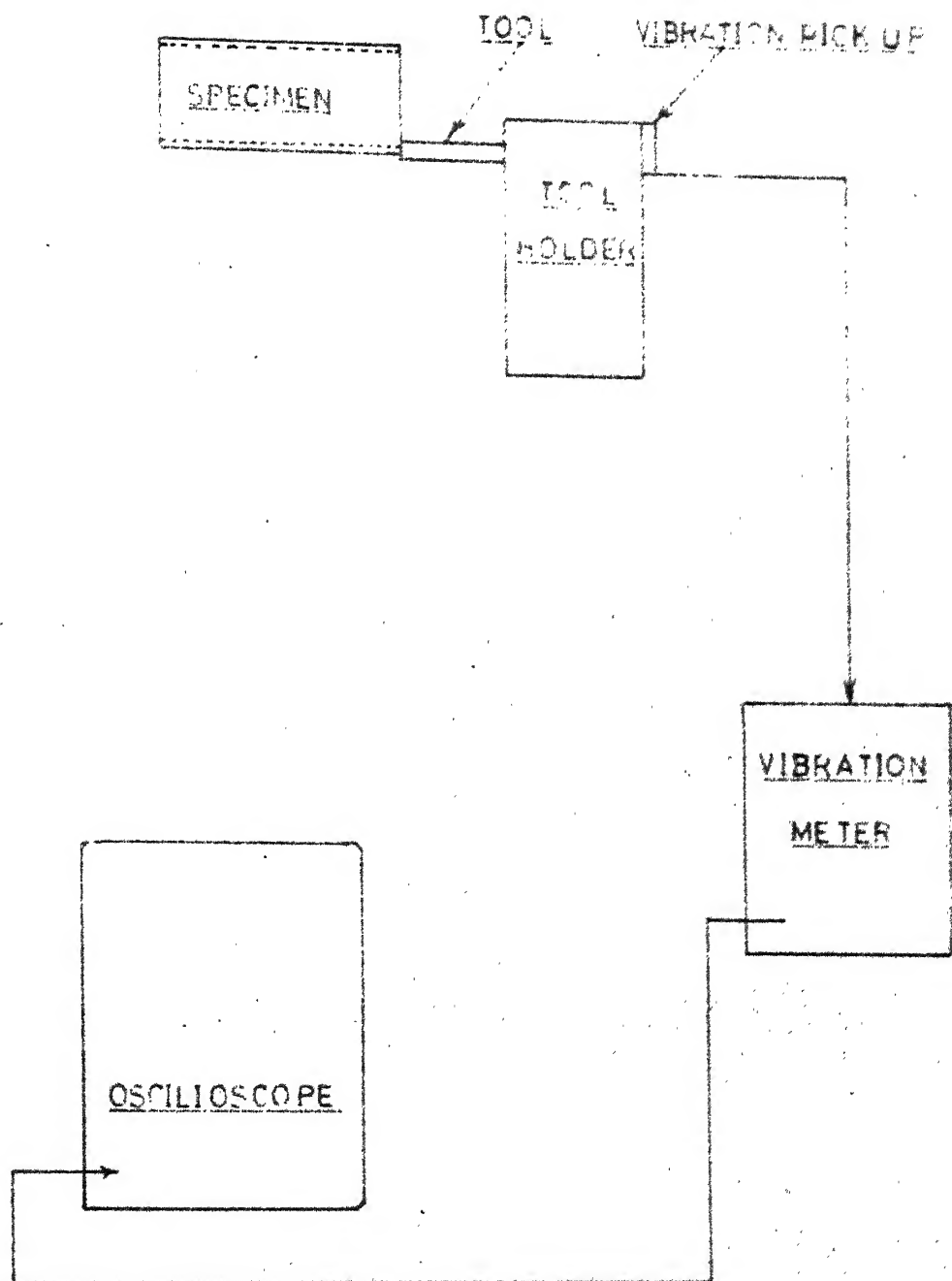
BLOCK DIAGRAM of SET UP FOR EXPERIMENTAL
STABILITY CHART

FIG.11

Thickness of the tube is varied from .5 mm to 1 mm in steps of
.1 mm after each set of tests for a range of cutting speeds
at a particular thickness.

Amplitude of vibration is measured by the help of
the vibration meter and the frequency of vibration is obtained
by displaying the signal on the storage oscilloscope. Fresh
cutting edge is used for each test. After every reading
the wavy surface left on the workpiece, by the previous
test, is removed by the help of back tool post. Three readings
are taken for each speed for a particular width of cut. Tests
are conducted for spindle speeds of 100 to 500 rp.m. in steps
of 20 rp.m.

Figure 12 shows plots of frequency versus revolutionary
speed. Width of cut is also plotted against speed. The upper
portion of the graph shows straight lines corresponding to
stability lobes. Stability lobes are drawn touching the points
showing stability such that all the points showing vibrations
lie above the boundaries of the lobes. An envelope to these
stability lobes is termed as threshold of stability curve.
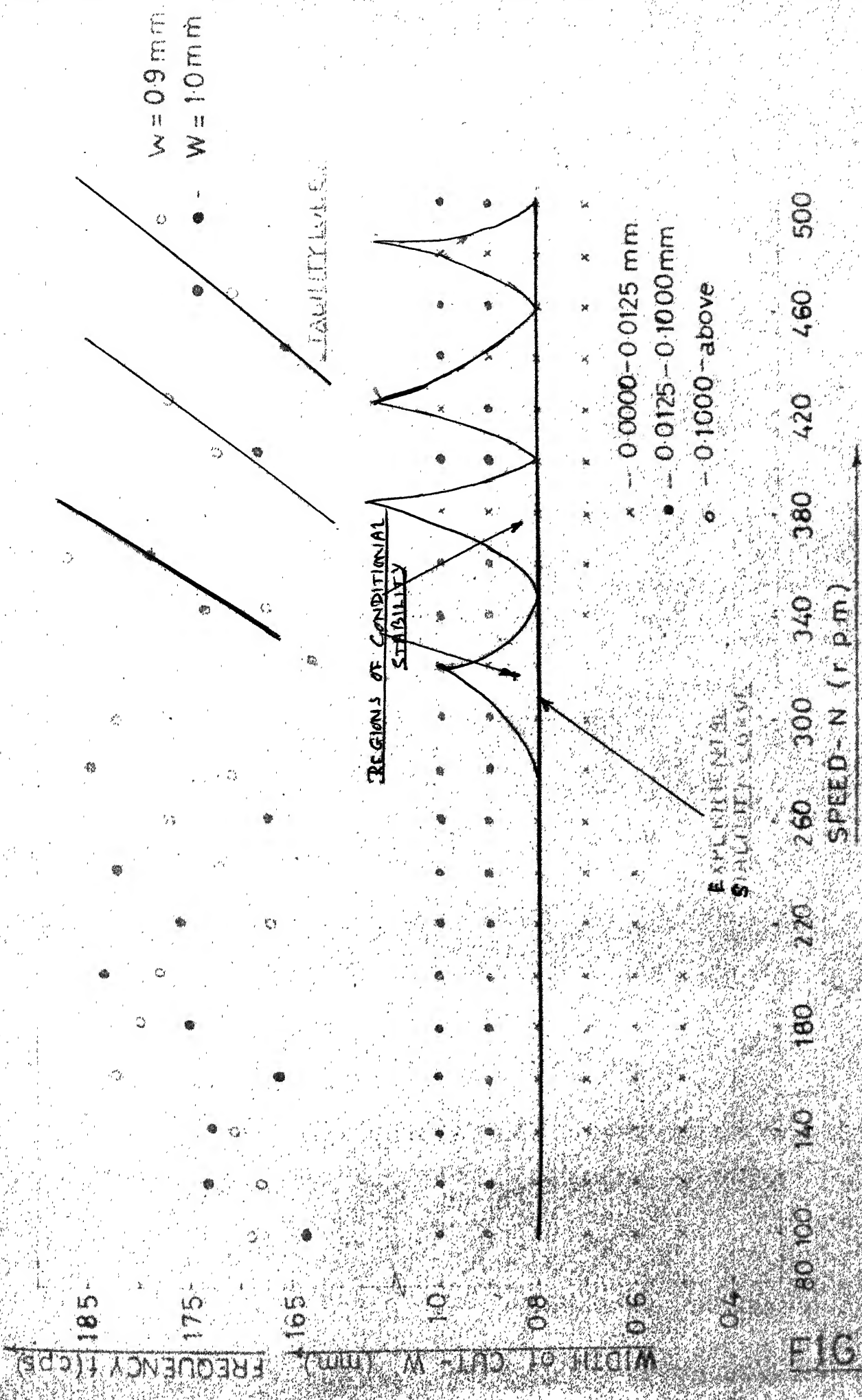
FIG 12

EXPERIMENTAL STABILITY CHART of THE TOOL HOLDER

SPEED- N (r.p.m)

80 100   140   180   220   260   300   340   380   420   460   500

WIDTH of CUT - W (mm)

0.4   0.6   0.8   1.0

Regions of CONDITIONAL STABILITY

x — 0.0000—0.0125 mm
● — 0.0125—0.1000mm
○ — 0.1000—above

STABILITY LINE

W = 0.9 mm
W = 1.0 mm

FREQUENCY f (cps)

165   175   185

THEORETICAL STABILITY CHART

3.1 Introduction

In the present study, machine tool system is assumed a simplified single degree of freedom system. Hence the cross receptance (p+iq) is taken zero. Also in orthogonal cutting value of overlap-factor μ is one. Hence for the present case equationsof the threshold of stability reduce to the following equation:,

$$\frac{1}{W} = - \frac{T_c}{\sin \emptyset} \left[\begin{array}{l} \{g(1-\cos \theta')-h \sin \theta'\}\{c-n_1 s(1+2c \cot \emptyset)\} \\ - \frac{h\omega s}{V} \{(1+c \cot \emptyset)-K_1(1+2c \cot \emptyset)\} \end{array} \right] \quad (3.1)$$

$$0 = \left[\begin{array}{l} \{h(1-\cos \theta') + g \sin \theta'\} \{c-n_1 s(1+2c \cot \emptyset)\} \\ + \frac{g\omega s}{V} \{(1+c \cot \emptyset) - K_1 (1+2c \cot \emptyset)\} \end{array} \right] \quad (3.2)$$

where,

$$\theta' = \frac{\omega}{n} (1 - \frac{s \cot \emptyset}{2 \pi r n}) \quad (3.3)$$

Theoretical stability chart can be predicted by solving the equations (3.1) and (3.2). For this purpose, response locus of the tool-holder and the variation of the following cutting parameters with cutting speed is required :

(a) Cutting stress T_c'

(b) Shear angle 'ϕ'

(c) Stress ratio 'D' and

(d) Shear angle coefficients n_1 and n_2.

Variation of 'T_c', 'D', 'n_1' and 'n_2' with cutting speed
_____

Kainth (Ref.8) has given graphs for the variation
of 'T_c', 'D', 'n_1' and 'n_2' with cutting speed. He also used
hot finished M.S. tube with .25% carbon and carbide tool with
5° rake angle. Cutting stress 'T_c', 'D' and 'n_2' are independent
of chip thickness (Ref.8) and their variation with cutting
speed is shown in Fig. 13 and 14. The variation of n_1 with
cutting speed for chip thickness of .05 mm is obtained by
intrapolating the results of Kainth (Ref.8). The intropolated
curve is shown in Fig. 14.

By using the multiple regression analysis, the
following polynomials are fitted to the curves given in
Figs. 13 and 14.

$$T_c = 2.48 + 15.14 \ (V/10) - 1.1 \ (V/10)^2 + .04(V/10)^3$$
$$- .00043 \ (V/10)^4$$

$$D = .768 + 1.14 \ (V/10) - .78 \ (V/100)^2 + .215 \ (V/100)^3$$
$$- .02 \ (V/100)^4$$
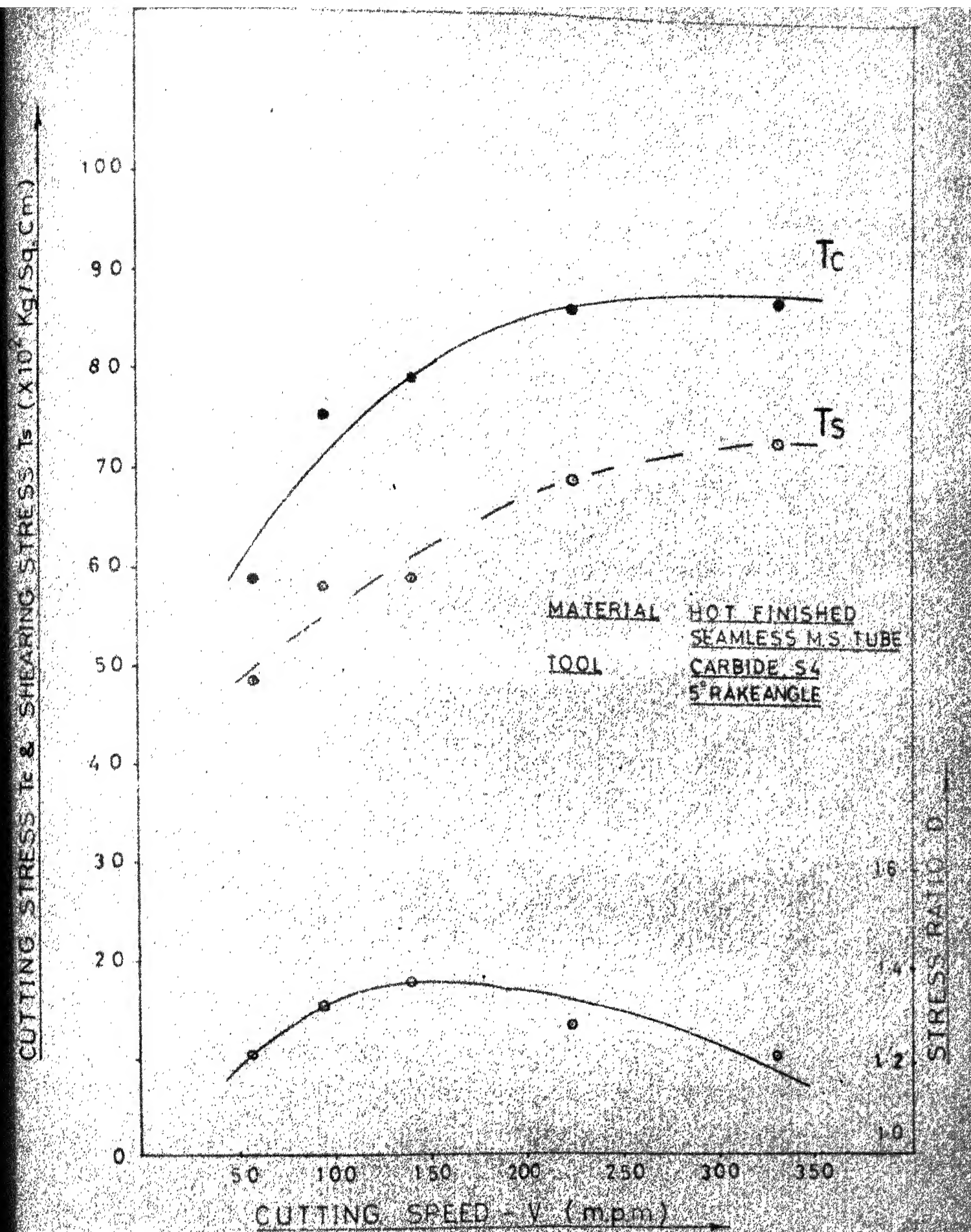
VARIATION of Tc, Ts & D WITH CUTTING SPEED

FIG.13
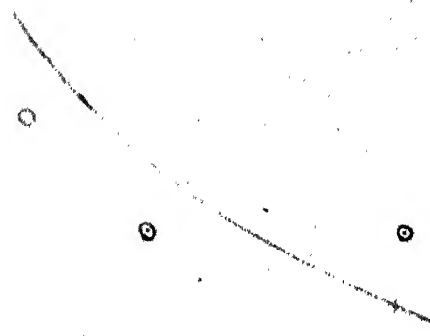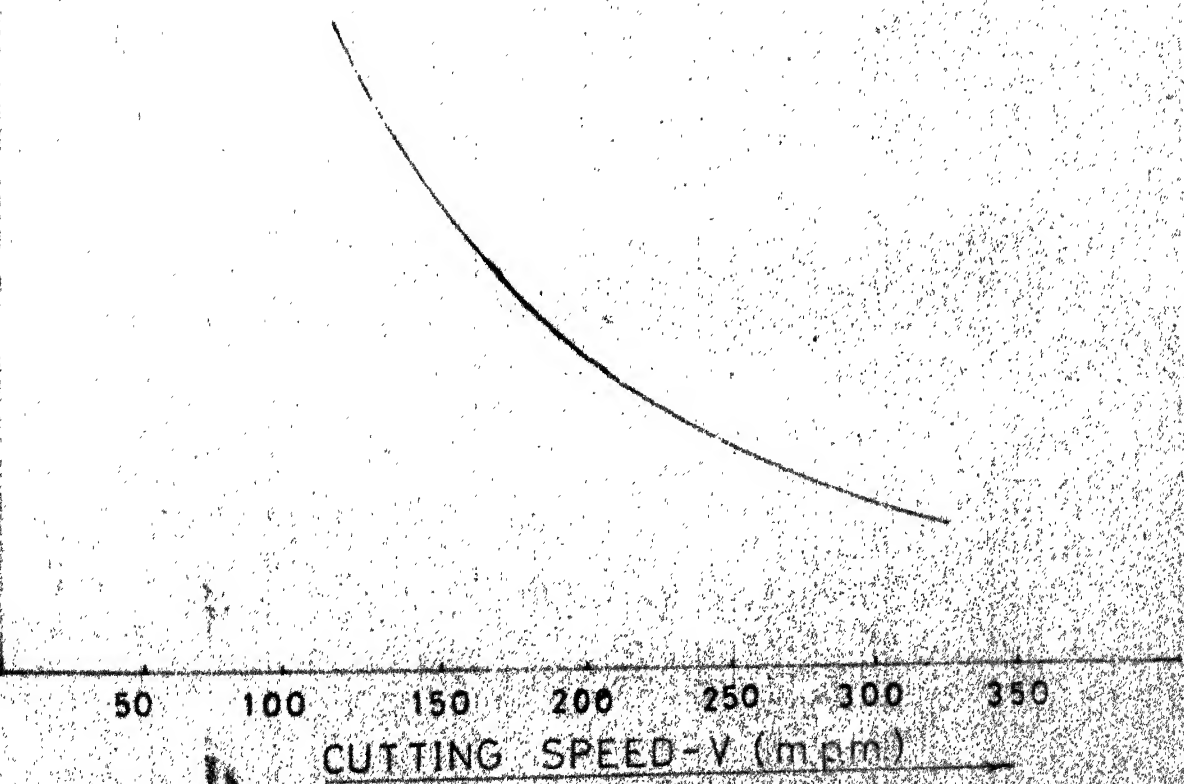
VARIATION of COEFFICIENTS n_1 & n_2 WITH CUTTING SPEED

FIG. 14

$$n_1 = 1.348 \ (V/100)^{-.2715}$$

$$n_2 = 3.4 \ (V \times 3.281)^{-.38}$$

where T_c = Cutting stress in kg/mm^2

          D = Stress Ratio

          n_1 = shear angle-chip thickness coefficient *radians/mm.*

          n_2 = shear angle-rake angle coefficient

          V = cutting velocity in m.p.m.

3.3 Variation of Shear Angle $\emptyset$ with Cutting Speed V

Experiments are carried out for determining the variation of shear angle with cutting speed.

Mild steel specimen is machined to give a mean radius of 54 mm and width of cut of 2.2 mm. Carbide tool with 5° rake angle is used for cutting. Feed of .05 mm/rev. is kept constant.

Method of length measurement is used to determine shear angle. A 'Vee' groove is cut on the tube, longitudinally. Chips collected during cutting carry nothes corresponding to the groove. Chips equivalent of 4 to 5 revolutions are collected and measured, thus giving the length of chip after machining. The notches on the chips collected are used to determine the number of revolutions of the work-piece during cutting.

Therefore initial uncut chip length L_1 is,

$$L_1 = 2 \pi r N$$

where   r = Mean radius of work piece

N = Number of revolutions for which chip length is

measured

If L_2 is the chip length measured, then the chip thickness
ratio 'r_c' is

$$r_c = \frac{s_1}{s_2} = \frac{L_2}{L_1}$$

and shear angle $\emptyset$ is,

$$\emptyset = \text{Arctan} \left(\frac{r_c \cos\alpha}{1 - r_c \sin\alpha} \right)$$

where α is the rake angle of the tool.

The variation of shear angle $\emptyset$ with cutting speed
is shown in Fig. 15.

The following second order polynomial is fitted to
the above curve,

$$\emptyset = 6.482 + .6813(V/10) - .0067 (V/10)^2$$

where $\emptyset$ is in degrees and V is in m.p.m.

3.4 Solution of the Equations of Threshold of Stability

For a particular frequency, roots of equation (3.2)
are determined and for these roots values of widths of cut
are calculated from equation (3.1).
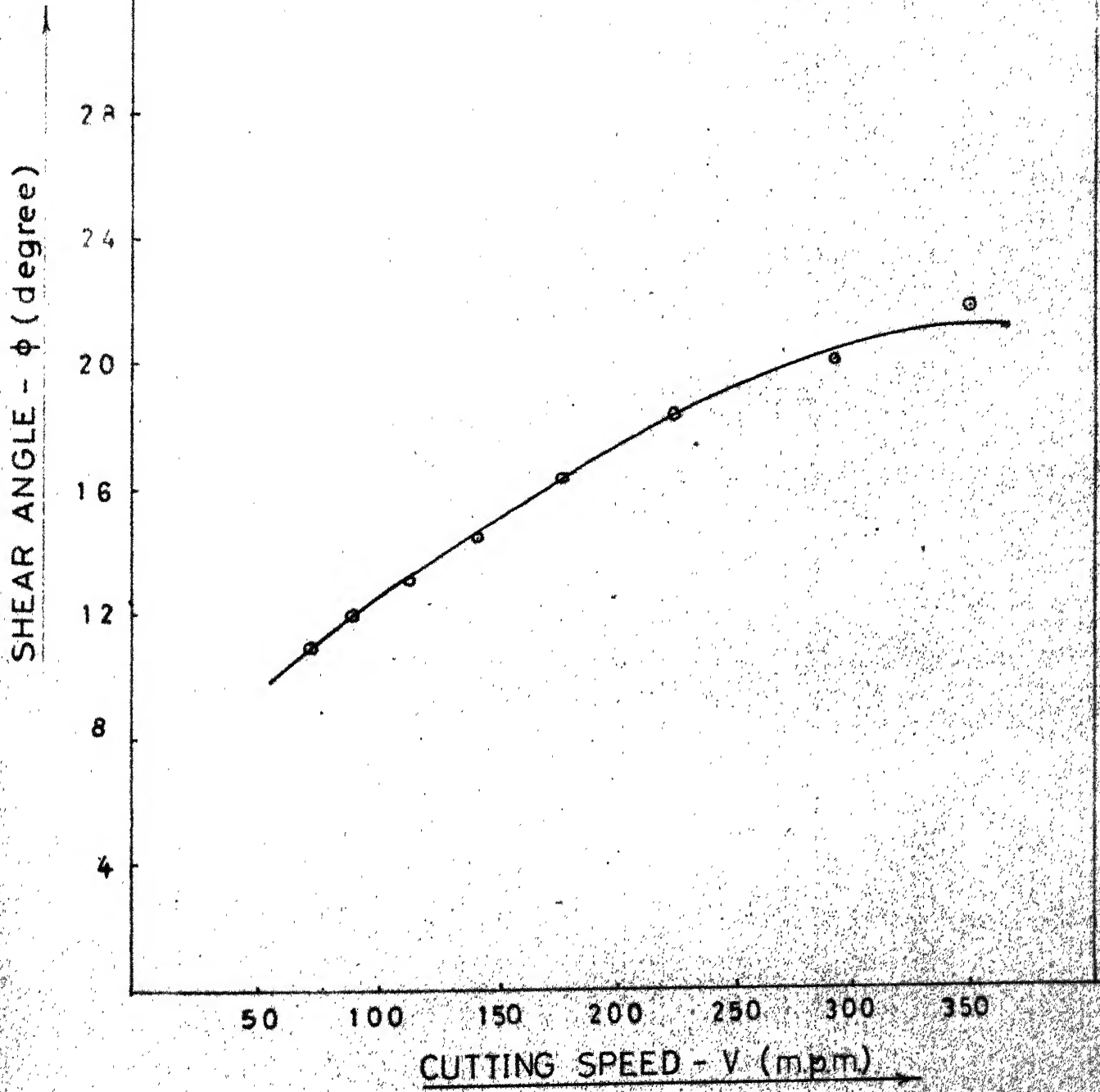
VARIATION of SHEAR ANGLE WITH CUTTING SPEED

FIG.15

A computer program is developed to solve equations (3.1) and (3.2). The program is given in Appendix.

Search for the roots of the equation 3.2 starts from 60 r.p.m. for a particular frequency. Frequency range of 160 c.p.s. to 230 c.p.s. is used in steps of 2.5 c.p.s. At these frequencies values of inphase and out of phase components a and b respectively is determined from the harmonic response locus of the tool-holder.

For a particular frequency function value of equation 3.2 is calculated, at steps of 0.3 r.p.m. At each of the steps values of cutting parameters $\emptyset$, D, n_1 and n_2 are taken from the fitted curves. Whenever, at two consecutive steps, the function value changes its sign, a root is expected in the step. Steefanson's search technique is used to determine the root where the function value approaches 10^{-5}. All the roots are searched for a frequency and the whole procedure is repeated for all frequencies.

Values of cutting parameters T_c, D, $\emptyset$, n_1 and n_2, at the roots determined from equation 3.2 is put in equation 3.2 and corresponding widths of cut are calculated.

The theoretical stability chart is shown in Fig. 16.

CHAPTER 4

DISCUSSION AND CONCLUSION

A comparison of the theoretical and the experimental stability charts is shown in Figure 17. Experimental stability chart is a straight line in the speed range of 100 to 500 rpm. Vibrations of amplitude lesser than .0125 mm are considered stable. The tool holder is stable upto a width of cut .8 mm. For widths of cut of .9 mm and 1.0 mm., vibrations are of considerable amplitude. At these widths of cut certain speeds are stable which lin in the stability regions above the envelope of threshold of stability. These stability regions are called regions of conditional stability.

Theoretical stability chart shows a rising trend for speeds lower than 200 rpm. Between 220 rpm. and 500 rpm. the theoretical stability chart is quite close to the experimental stability chart, the maximum deviation being 12.5%.

At lower cutting speeds below 200 rpm, the theoretical values are higher than the experimental values. The reason is that Kainth's (Ref.8) theoretical analysis is not applicable for the built up edge conditions which is obtained below cutting velocity of 60 m.p.m. (180 r.p.m. in the present case). However in practice carbide tools are used at cutting velocity

higher than 100 m.p.m. (300 r.p.m.), where the theoretical analysis shows fairly good agreement with the experimental results.

It is concluded that the dynamic shear angle approach is adequate to predict the threshold of stability of machine tool system.

REFERENCES

1. Tobias, S.A.

   "Machine Tool Vibrations", Blackie
   and Son Ltd., 1965.

2. Sweeney, G.
   and Tobias, S.A.

   "An Algebric Method for the Determina-
   tion of the Dynamic Stability of
   machine Tools". Proc. Int. Conf.
   Res. Prod. Engg. Phttsburg, 1963,
   p. 475, ASME, New York.

3. Tlusty, J. and
   Polacek, M.

   "Theorie der Selbsterrgten Schwingungen
   bei der Zerspannung und die Stabilita-
   tsberechung der Werkzeugmaschinen",
   Industrie Anzeiger, No. 28, 1957, p.395.

4. Tobias, S.A. and
   W. Fishwick

   "Theory of Regenerative Machine Tool
   Chatter", The Engineer, Vol. 205,
   1958, p. 199.

5. Das, M.K.

   "Physical Aspects of the Dynamic
   Cutting of Metals", Ph.D. Thesis.
   University of Birmingham, 1965.

6. Das, M.K. and
   Tobias, S.A.

   "The Rolation between the Static
   and Dynamic Cutting of Metals",
   Int. J. Mech. Tool Des. Res., 1967,
   Vol. 7, p. 63.

7. Knight, W.A.   "Torsional Vibration and Machine
                   Tool Stability", Ph.D. Thesis,
                   University of Birmingham, 1967.

8. Kainth, G.S.   "Investigation into the Dynamics of
                   the metal Cutting Process", Ph.D.
                   Thesis, University of Birmingham, 1969.

9. Loomba, K.M.   "Experimental Investigation into the
                   Dynamic Response of Lathe-bed", M.Tech.
                   Thesis, Dept. of Mech. Engg., I.I.T.
                   Kanpur, 1971.

APPENDIX

```
          THIS PROGRAM IS TO SOLVE THE EQUATIONS OF THRESHOLD OF STABILITY
$IBJOB
$IBFTC MAIN
          REAL N1,N2,N,K1
          DIMENSION FF(30),GG(30),HH(30),ROOT(500),WW(500)
          COMMON /VISHNU/THETA,K1,C,V,FI,S,N1,OMEGA,H,F,GSMALL
          COMMON /BLOCK /ROOT,M
  500     FORMAT(1X,10F10.3)
  510     FORMAT(1X,*FREQUEJENCY*,3F10.3)
  110     FORMAT(8F10.1)
  210     FORMAT(8F10.6)
          READ110,(FF(I),I=1,30)
          READ210,(GG(I),I=1,30)
          READ210,(HH(I),I=1,30)
          DO 100 I=1,30
          F=FF(I)
          GSMALL=GG(I)
          H=HH(I)
          XMIN=2.0
          XMAX=10.0
          STEP=.005
          EPS=1.*E-06
          CALLSTEEF(XMIN,XMAX,STEP,EPS)
          DO 10 J=1,M
          X=ROOT(J)
          CALL FUNC(X,F1)
          V1=V/1000.*60.
          TC=10.*(.247856+1.51426*V1/10.-.10981*(V1/10.)**2+.00358*(V1/10
     1    .)**3-.00004273*(V1/10.)**4)
          W=-SIN(FI)/TC/((GSMALL*(1.-COS(THETA))-H*SIN(THETA))*( C-N1*S*Y1
     1    .+2.*C/TAN(FI)))-H*OMEGA*S/V*((1.+C/TAN(FID)-K1*(1.+2.*C/TAN(FI))))
          WW(J)=W
          ROOT(J)=ROOT(J)*60.
   10     CONTINUE
          PRINT510,GSMALL,H,F
          PRINT500,(ROOT(J),J=1,M)
          PRINT500,(WW(J),J=1,M)
  100     CONTINUE
          STOP
          END
$IBFTC FUNC
          SUBROUTINE FUNC(N,FF)
          REAL N1,N2,K1,N
          COMMON /VISHNU/THETA,K1,C,V,FI,S,N1,OMEGA,H,F,GSMALL
          PI=4.*ATAN(1.0)
          FD(X)=.768+1.14363*X/100.-.78183*(X/100.)**2+.2155*(X/100.)
     1    **3-.021694*(X/100.)**4
```

52

```
          FIA(X)=6.482+.68127*(X/10.)-.006668*(X/10.)**2
          FN1(X)=1.348*(X/100.)**(-.2715)
          FN2(X)=3.4*(X*3.281)**(-.38)
          R=54.0
          S=.05
          V=2.*PI*R*N
          V1=V/1000.*60.
          N2=FN2(V1)
          N1=FN1(V1)
          FI=FIA(V1)*PI/180.
          D=FD(V1)
          G=S/TAN(FI)
          K1=G*N1+N2
          C=(D*COS(FI)-1.)/D/SIN(FI)
          OMEGA=2.*PI*F
          THETA=OMEGA/N*(1.-S/TAN(FI)/2./PI/R)
          FF=((H*(1.-COS(THETA))+GSMALL*SIN(THETA))*(C-N1*S*(1.+2.*C/TAN(FI))
     1    ))+GSMALL*OMEGA*S/V*((1.+C/TAN(FI))-K1*(1.+2.*C/TAN(FI))))
          RETURN
          END
$IBFTC STEEF
          SUBROUTINE STEEF(XMIN,XMAX,STEP,EPS)
C         PROGRAM IS FOR FINDING THE ROOTS OF TRANSCIDENTAL EQATION IN THE
C         GIVEN RANGE ITERATION FUNCTION USED REQUIRES NO DERAVATI() EVALU
C         NOTATION USED ARE
C         XMIN=MINIMUM VALUE OF INDEPANDENT VARIABLE               *
C         XMAX=MAXIMUM VALUF OF INDEPANDENT VARIABLE               *****
C         STEP=STEP SIZE USED FOR SEARCHING THE VICINITY OF THE ROOT *****
C         ATION STILL CONVERGENCE IS FASTER THEN NEWTON'S METHOD    *****
C         EPS=ACCURACY DESIRED FOR THE FUNCTION                    *****
          DIMENSION ROOTS(500),FUNCTN(500)
          COMMON/BLOCK/ROOTS,M
  100     FORMAT(10X,*NO. OF SOLUTION HAS EXCEEDED 20 *)
  101     FORMAT(10X,I4,2F12.5)
  102     FORMAT(10X,*SORRY NO SOLUTION IN THE GIVEN RANGE *)
  103     FORMAT(10X,*SOLUTION BY STEFFENSON'S IMPROVED REGULA FALSI METHO
     1    D*//,10X,* NO.*5X,*ROOTS',7X,*FUNCTION*//)
C         SEARCH FOR THE VICINITY 6F THE ROOT *****************************
          X1=XMIN
          CALL FUNC(X1,F1)
          M=0
          IF(ABS(F1).GT.EPS)GOTO10
C         IS SEARCH POINT VERY CLOSE TO THE ROOT *************************
          X=X1
          F=F1
          X2=X+5.*EPS
          CALL FUNC(X2,F2)
          GOTO40
  10      CONTINUE
          X2=X1+STEP
          CALL FUNC(X2,F2)
C         IS SEARCH POINT VERY CLOSE TO THE ROOT *************************
          IF(ABS(F2).GT.EPS)GOTO20
          X=X2
```

```
          F=F2
          X2=X+5.*EPS
          CALL FUNC(X2,F2)
          GOTO40
   20     CONTINUE
          IF(F1*F2.LT.0.0)GOTO30
          GOTO50
   30     CONTINUE
          CALL REGULA(X1,X2,F1,F2,EPS,X,F)
   40     CONTINUE
          M=M+1
          IF(M.EQ.20)PRINT100
          ROOTS(M)=X
          FUNCTN(M)=F
C         IF(M.EQ.20)PRINT101,(I,ROOTS(I),FUNCTN(I),I=1,20)
C         IF(M.EQ.20)M=0
C         SEARCH FOR THE NEXT ROOT STARTS ********************************
   50     CONTINUE
          X1=X2
          F1=F2
C         TEST FOR THE SEARCH DOMAIN EXOUSTED OR NOT *******************
          IF(X1.LT.XMAX)GOTO10
          IF(M.EQ.0)PRINT102
          IF(M.GT.0)PRINT103
C         IF(M.GT.0)PRINT101,(I,ROOTS(I),FUNCTN(I),I=1,M)
          RETURN
          END
$IBFTC REGULA
          SUBROUTINE REGULA(X1,X2,F1,F2,EPS,X3,F3)
  100     FORMAT(10X,*NOT CONVERGING IN 30 ITERATION */)
  101     FORMAT(10X,*ITERATION NO.*,I3)
  102     FORMAT(10X,8F8.4)
C         STEFFENSON'S IMPROVED REGULA FALSI ITERATION FUNCTION    *****
C         THIS ITERATION FUNCTION IS OF THE ORDER OF 3.23 REQUIRS NO *****
C         DERIVATIVE EVALUATION.  FUNCTION IS WITH MEMORY **************
          M=1
   10     CONTINUE
          X3=(X1*F2-X2*F1)/(F2-F1)
          IF(F1*F2.LT.0.0)X3=(X1*X3-X2**2)/(X1-2.*X2+X3)
          CALL FUNC(X3,F3)
          IF(ABS(F3).LT.EPS)GOTO60
          IF(M.EQ.30)GOTO50
   20     CONTINUE
C         PRINT102,X1,F1,X2,F2,X3,F3
          IF(F1*F3.LT.0.0)GOTO30
          X1=X3
          F1=F3
          GOTO40
   30     CONTINUE
          F2=F3
```

```
         X2=X3
  40     CONTINUE
         M=M+1
         GOTO10
  50     CONTINUE
C        PRINT100
  60     CONTINUE
         X2=X3+5.0*EPS
         CALL FUNC(X2,F2)
C        PRINT101,M
         RETURN
         END
  $ENTRY
```

13